ATOMIZATION CHARACTERISTICS OF FLAT FAN NOZZLES FOR PRECISION PESTICIDE APPLICATION AT LOW PRESSURES
/
针对精准施药的平扇形喷嘴低压雾化特性

Shougen Li, Yaxiong Wang, Chongchong Chen, Feng Kang*), Wenbin Li [1]
School of Technology, Beijing Forestry University, Key Lab of State Forestry Administration for Forestry Equipment and Automation, Beijing, 10083, China;
**Tel: 13002515042; E-mail: kangfeng98@bjfu.edu.cn*
DOI: https://doi.org/10.35633/inmateh-61-32

Keywords: *flat fan nozzle, spray axis, droplet velocity, droplet size*

ABSTRACT

At present, the theory of precision pesticide application in agriculture and forestry has some shortcomings. Therefore, the Phase Doppler Interferometer (PDI) was used to establish the atomization model of three common brands (Lechler, Teejet and Feizhuo) flat fan nozzles in near fog field (0.3-0.5m) at low pressure (0.20-0.30mPa). The results show that the average absolute errors of droplet velocity of three brands of nozzles are 0.629, 0.521 and 0.684 m/s respectively, and the relative errors are 9.22, 9.60 and 11.89%, respectively. The average absolute errors of theoretical data of droplet size are 17.821, 13.801 and 22.140 μ m, and the relative errors are 8.40, 5.82 and 11.67%, respectively. The experimental theoretical model has high reliability. In addition, the results show that the droplet velocity and particle size increase with the increase of the equivalent diameter of the nozzle outlet. With the increase of spray angle, droplet velocity and particle size decrease gradually, and the rate of velocity decrease gradually. The research results are of great significance to further analyse the atomization characteristics of flat fan nozzle and guide the precise application of pesticide.

摘要

目前，农林精准施药理论理论存在不足。因此，本研究利用相位多普勒干涉仪（PDI）建立了低压（0.20-0.30mpa）下近雾场（0.30-0.50m）三种常用品牌（Lechler、Teejet 和 Feizhuo）平扇形喷嘴的雾化模型。结果表明，三种品牌喷嘴液滴速度理论数据的平均绝对误差分别为0.629、0.521 和0.684 m/s，相对误差分别为 9.22、9.60 和 11.89%。液滴粒径理论数据的平均绝对误差分别为 17.821、13.801 和 22.140μm，相对误差分别为 8.40、5.82 和 11.67%。理论模型非常可信。此外，结果表明，液滴速度和粒径随喷嘴出口等效直径的增大而增大。随着喷雾角度的增大，液滴速度和粒径逐渐减小，且速度降低率逐渐减小。研究结果对进一步分析平风扇喷嘴的雾化特性、指导精准施药具有重要意义。

Nomenclature

a_m	Constant
a_v	Constant
b_m	Constant
b_v	Constant
C	Constant
C_D	Constant
c_m	Constant
C_m	Constant
c_v	Constant
C_V	Constant
d_m	Constant
d	Equivalent orifice diameter (mm)
D	Droplet size (μm)
D_{max}	Maximum droplet size (μm)
D_{min}	Minimum droplet size (μm)
Dv	Volume median diameter (μm)
g	Gravity acceleration (m/s^2)
K	Constant
n	Constant
N	Quantity of droplets
P	Pressure difference of nozzle and outlet (Pa)
r_{in}	Radius of nozzle inlet (mm)
r_{out}	Radius of nozzle outlet (mm)
u	Liquid velocity (m/s)
u_m	Spray axis droplet velocity (m/s)
u_{max}	Maximum droplet velocity (m/s)
u_{min}	Minimum droplet velocity (m/s)
u_{in}	Velocity of nozzle inlet (m/s)
u_{out}	Velocity of nozzle outlet (m/s)
U	Average droplet velocity (m/s)
z	Coordinate value (m)
α	Spray angle (°)
σ_l	Droplet surface tension coefficient
ρ_l	Water density (kg/m^3)
ρ_g	Gas density (kg/m^3)

[1] *Shougen Li, As. PhD. Eng.; Yaxiong Wang, As. PhD. Eng.; Chongchong Chen, As. PhD. Eng.; Feng Kang, As. PhD. Eng.; Wenbin Li, As. PhD. Eng.*

INTRODUCTION

Spraying is an important method for pest control in agriculture and forest. For killing the pests with the habit of up and down migration along the trunk, Kang developed an automatic targeted application system using a barrier treatment and then improved the spray system (Fig. 1). Additionally, spray characteristics, the addition of adjuvants, pulse width modulation technology, and electrostatic spray have also attracted much attention. Spray characteristics mainly include two factors: droplet velocity and size. Droplets with appropriate velocities and size are not easy to drift and rebound, and have good deposition and coverage effects (*Wang S. et al., 2018; Patel M K et al., 2017; Preftakes C J et al., 2019*).

Fig. 1 - The spray system of forest barrier treatment

Current research on the distributions of droplet velocity and size has mostly focused on the industrial field. For example, Cui developed the microhole-measuring system based on a twin fibre Bragg grating (FBG) probe and obtained that small geometric differences had a significant effect on cavitating flow. Ghate studied the effect of orifice divergence on the spray characteristics of hollow cone nozzles. Results revealed that liquid film thickness and the axial and radial velocities at the orifice exit were drastically affected by divergence angle (*Ghate K., Sundararajan T. 2019*). Additionally, Geng found that the length-diameter ratio (L/D) of the nozzle inner structure's parameters had less of an impact than spray pressure or fuel temperature on the spray characteristics (*Geng L et al., 2020*). Moreover, studies on the spray characteristics have also been reported in the dust reduction (*Wang J et al., 2019*), food (*Chen G et al., 2018*), and cleaning industries. In agriculture and forestry, spray characteristic studies are less reported. Based on the assumption that the spray field is a 2D plane, Kang established the droplet velocity and size model by simulation and actual experiments (*Kang F et al., 2011*). A computational fluid dynamics (CFD) model was developed by Musiu to evaluate the distribution of droplet velocity and size at different settings for a greenhouse air blast sprayer, which predicted the actual measuring droplet size value.

Flat fan nozzles are the main nozzle in agriculture and forest. The atomization field of a flat fan nozzle is as shown in Fig. 2. In order to clearly describe it, a rectangular coordinate system in space was established with a nozzle exit centre as the coordinate origin. The X, Y, and Z axes were the long and short axes of the spray cross-section and spray axis, respectively. The shape of the 3D spray cross-section of the fan nozzle is approximately elliptical, which is basically symmetrical along the long and short axes. The spray characteristics of atomization field could be reflected by the distribution of droplet velocity and size along one spray line starting from the nozzle outlet.

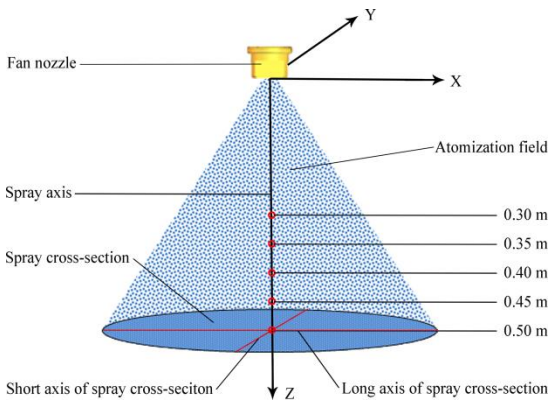

Fig. 2 - The atomization field of a flat fan nozzle. Red circles represent the measurement points

In this context, this study was to analyse the atomization characteristics of flat fan nozzles for agriculture and forest. The main relevant parameters were analysed at low pressures (0.20–0.30 MPa). A Phase Doppler Interferometer (PDI) was used for measuring all data at spray distances ranging from 0.30 to 0.50 m. Based the jet theory, this research improved and established the droplet velocity and size models, and provided guidance for agriculture and forest.

MATERIALS AND METHODS

Selection of nozzle type

Currently, the mainstream brands of flat fan nozzles in the market include Teejet (USA), Lechler (Germany), and Feizhuo (China), which are widely used in surface treatments, the food industry, agricultural and forestry pesticide application, and other fields. To identify similarities between these three brands, the Teejet TP, Lechler 632, and Feizhuo H/U flat fan nozzle series were selected for experimental measurements. In this study, the spray angles of 25°, 40°, 65°, and 80° for the Teejet and Feizhuo nozzles and 30°, 45°, 60°, and 90° for the Lechler nozzle were utilized as test objects (Table 1).

Table 1

The types of nozzles used in this study

α	Manufacturer	d			
		0.70	1.00	1.35	1.65
30	Lechler	632.302.30	632.362.30 [a]	632.442.30 [b]	632.512.30
45		632.303.30 [a]	632.363.30 [a]	632.443.30 [a]	632.513.30 [a]
60		632.304.30 [b]	632.364.30 [a]	632.444.30 [b]	632.514.30 [b]
90		632.306.30	632.366.30 [a]	632.446.30 [b]	632.516.30
α	Manufacturer	d			
		0.80	1.00	1.20	1.40
25	Teejet	2502	2503 [a]	2504 [b]	2505
40		4002 [a]	4003 [a]	4004 [a]	4005 [a]
65		6502 [b]	6503 [a]	6504 [b]	6505 [b]
80		8002	8003 [a]	8004 [b]	8005
α	Manufacturer	d			
		0.91	1.10	1.30	1.40
25	Feizhuo	2502	2503 [a]	2504 [b]	2505
40		4002 [a]	4003 [a]	4004 [a]	4005 [a]
65		6502 [b]	6503 [a]	6504 [b]	6505 [b]
80		8002	8003 [a]	8004 [b]	8005

[a] *Nozzles used to establish the model.*

[b] *Nozzles used to verify the established model.*

Abbreviated forms were used as type names in the following text, for example, 632.302.30-302, where 30 and 2 represent the flow rate and spray angle in the abbreviated Lechler, respectively, and 25 and 02 represent the spray angle and flow rate for Teejet and Feizhuo, respectively. Flow rate was determined by the equivalent orifice diameter. The Lechler, Teejet, and Feizhuo nozzles are hereafter referred to as LN, TN, and FN, respectively.

Theoretical basis

The findings of this study will serve the agricultural and forestry pesticide application. Droplet velocity and size are expressed by the average velocity and volume mean diameter (VMD), respectively.

The formulas are as follows:

$$U = (\int_{u_{\min}}^{u_{\max}} u_d dN) / (\int_{u_{\min}}^{u_{\max}} dN) \quad (1)$$

$$D_v = ((\int_{D_{\min}}^{D_{\max}} D^3 dN) / (\int_{D_{\min}}^{D_{\max}} dN))^{1/3} \quad (2)$$

The pressure (P), spray distance (z), spray angle (α), and equivalent orifice diameter (d) are the main factors that affect axial velocity and size *(Kooij S. et al., 2018)*. Therefore, this study analysed and discussed these factors to establish an axial atomization model for flat fan nozzles.

Assuming that these factors are independent, the function of the axial atomization model was established as follows:

$$u_m, D_v = f(z) f(P) f(d) f(\alpha) \quad (3)$$

For the incompressible flow in the nozzles, pressure and velocity satisfied the Bernoulli formula, as follows:

$$(P / \rho_l) + gz + (u^2 / 2) = K \quad (4)$$

For a given nozzle, the internal flow velocity was inversely proportional to the square of the inner diameter.

The formula is as follows:

$$u_{in} / u_{out} = r_{out}^2 / r_{in}^2 \quad (5)$$

After ejection, liquid film was mainly affected by liquid flow characteristics, gas-liquid two-phase physical properties, and flow conditions. Due to disturbances in the external gas, droplet groups were finally formed after breakage. Sforza proposed that the 3D spray axial velocity is negatively and exponentially decremented by spray distance (*Sforza P M et al., 1966*).

The formula is as follows:

$$u_m = x^{-n} \quad (6)$$

For the flat fan nozzles used in this study, velocity changes caused by gravity and nozzle inlet velocity were negligible. The spray axial velocity was obtained from formulas (3–5):

$$u_m = \left(2P / \rho\right)^{0.5} z^{-a_m} \quad (7)$$

Thus far, only a few theoretical studies on the droplet size distribution of flat fan nozzles using 2D and 3D sprays have been reported. Hinze (*Hinze J. O. 1955*) validated the relationship between droplet velocity and size in a steady state using experimental and theoretical approaches.

The formula is as follows:

$$D_{\max} = (8\sigma_l) / (C_D \rho_g u^2) \quad (8)$$

For a given nozzle, the VMD of the droplets was related to the spray pressure and flowrate of the liquid (*Jiang Y. et al., 2019*). Based on this information, Kang obtained the relationship between the average VMD of the atomization field and spray pressure (*Kang F et al., 2018*).

The formula is as follows:

$$D_v = C\Delta P^{-1/3} \quad (9)$$

Therefore, the functional form of axial droplet size would be similar to the functional form of axial droplet velocity.

Experimental design

Tests were conducted in the Laboratory of Agricultural Aviation Aerodynamics, Beijing Academy of Agriculture and Forestry Sciences, China. A laser PIII-X00MD PDI was used to collect data on droplet velocity and size of the atomization field. A 1WZB-25Z PRODN pressure pump was utilized to supply stable pressure for the measuring system, and a 3DOF mobile platform was used to precisely control the PDI position.

The system also included flow meters, pressure gauges, nozzle holders, and a liquid circulatory system (Fig. 3).

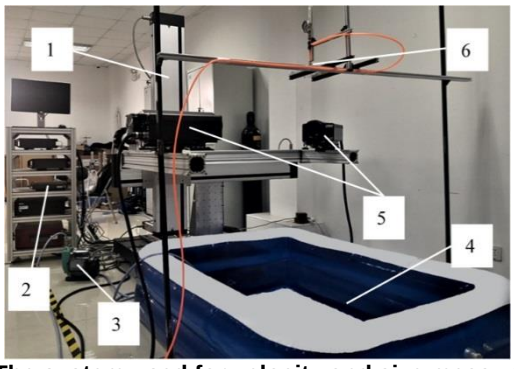

Fig.3 - The system used for velocity and size measurements

(1) 3DOF mobile platform; (2) Control centre; (3) Pump; (4) Liquid circulatory system; (5) PDI; (6) Flat fan nozzle

This study investigated a basic drop velocity and size model. Tests were conducted indoors with no wind at a stable temperature (18°C–22°C) and humidity (40%–60% RH) so that droplet evaporation could be ignored. In order to minimize the influence of gravity, nozzles were directed vertically downward. Five measuring points were selected along the Z-axis ranging from 0.30 to 0.50 m at 0.05 m intervals (Fig. 2). The preset pressures were 0.20, 0.25, and 0.30 MPa. Three replicates were conducted at each measurement point, and at least 5000 droplets were measured per replicate to ensure the accuracy of measurement data. Droplet velocities and sizes at the measurement points were thereby obtained.

Axial droplet velocity and size data were acquired using an Automated Instrument Management System (AIMS) software. Origin 2018 was used to draw the best-fit curves for droplet velocity and size of different factors.

RESULTS

Establishment of the droplet velocity model

The spray axial velocities at different distances of 18 selected nozzles were investigated (Fig. 4). The spray axial velocity at three spray pressures gradually decreased as spray axial distance increased, which was due to the kinetic energy gradually being reduced and the droplet velocity, thereby being reduced due to air resistance. Additionally, the velocity reduction rate gradually decreased as spray axial distance increased. This phenomenon was a result of the air resistance of droplets being inversely proportional to the square of its velocity; the lower the droplet velocity, the smaller the resistance. The mathematical functions of the best fit curve of axial velocity and spray distance for the three brands of nozzles were obtained as follows:

$$u_m = z^{a_m} \tag{10}$$

Where a_m was -0.58 for LN and -0.55 for TN and FN. Fitting degrees of the spray axial velocity and spray axial distance are provided (Table 2).

Table 2

Fitting degrees of spray axial velocity and distance

Parameter	LN 362	LN 363	LN 443	LN 513	LN 364	LN 366
R^2	0.996	0.997	0.998	0.946	0.981	0.997
Parameter	TN 2503	TN 4003	TN 4004	TN 4005	TN 6503	TN 8003
R^2	0.997	0.981	0.993	0.998	0.908	0.980
Parameter	FN 2503	FN 4003	FN 4004	FN 4005	FN 6503	FN 8003
R^2	0.996	0.999	0.997	0.993	0.951	0.986

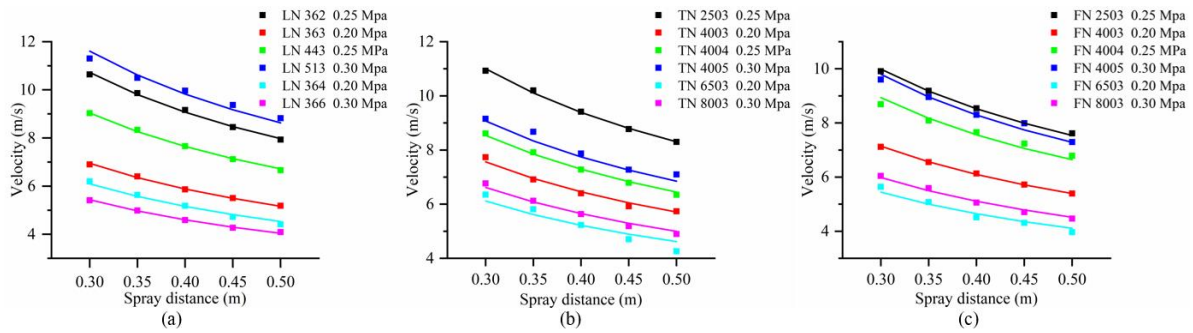

Fig. 4 - The relationship between axial velocity and spray distance

Results revealed that the spray axial velocities decreased as spray angle increased among the 15 nozzles from the three brands (Fig. 5). That was because droplets were more affected by air resistance at the same flow rate, as spray width increased with the increase of the spray angle. The relationship between the spray angle and axial velocity by fitting satisfied the following function:

$$u_m = \exp(b_m + c_m / \alpha) \tag{11}$$

Where b_m and c_m were 1.14 and 32.16 for LN, and 1.34 and 21.41 for TN and FN, respectively. Fitting degrees of the spray axial velocity and angle are provided (Table 3).

Table 3

Fitting degrees of spray axial velocity and spray angle

Parameter	LN 0.30 m	LN 0.35 m	LN 0.40 m	LN 0.45 m	LN 0.50 m
R^2	0.988	0.994	0.996	0.995	0.998
Parameter	TN 0.30 m	TN 0.35 m	TN 0.40 m	TN 0.45 m	TN 0.50 m
R^2	0.985	0.980	0.998	0.993	0.989
Parameter	FN 0.30 m	FN 0.35 m	FN 0.40 m	FN 0.45 m	FN 0.50 m
R^2	0.987	0.993	0.989	0.988	0.991

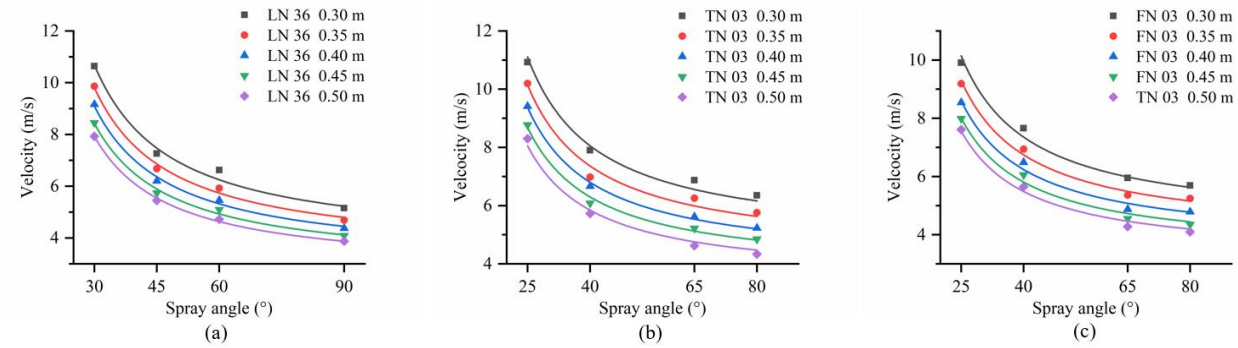

Fig. 5 - The relationship between axial velocity and spray angle

Axial velocity increased as the equivalent orifice diameter increased at a spray angle of 45° for LN and 40° for TN and FN (Fig. 6).

The relationship between the equivalent orifice diameter and spray axial velocity by fitting satisfied the following function:

$$u_m = d^{d_m} \tag{12}$$

Where d_m was 0.66 for LN, 0.60 for TN and 0.80 for FN. Fitting degrees of the spray axial velocity and equivalent orifice diameter are provided (Table 4).

Table 4

Fitting degrees of spray axial velocity and equivalent orifice diameter

Parameter	LN 0.30 m	LN 0.35 m	LN 0.40 m	LN 0.45 m	LN 0.50 m
R^2	0.980	0.949	0.966	0.964	0.957
Parameter	TN 0.30 m	TN 0.35 m	TN 0.40 m	TN 0.45 m	TN 0.50 m
R^2	0.946	0.979	0.956	0.972	0.983
Parameter	FN 0.30 m	FN 0.35 m	FN 0.40 m	FN 0.45 m	FN 0.50 m
R^2	0.988	0.990	0.983	0.970	0.981

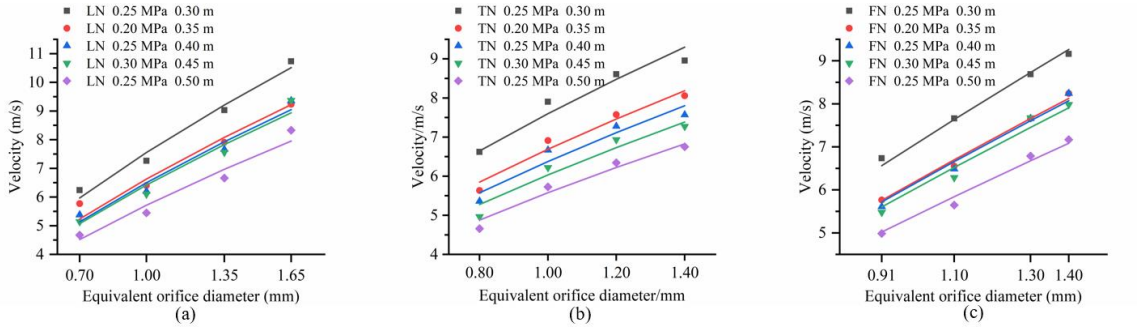

Fig. 6 - The relationship between droplet size and equivalent orifice diameter

By combining formulas (10)–(12), the spray axis velocity formula was established as follows:

$$u_m = \left(2P/\rho\right)^{0.5} z^{a_m} \exp(b_m + c_m/\alpha) d^{d_m} \quad (13)$$

The parameter values of the three different nozzle brands in the formula are provided (Table 5).

Table 5

Parameter values of the droplet velocity formula

Parameter	LN	TN	FN
a_m	-0.58	-0.55	-0.55
b_m	1.14	1.34	1.34
c_m	32.16	21.41	21.41
d_m	0.66	0.60	0.80

Establishment of the droplet size model

No noticeable changes were observed in the droplet size between the six nozzles of each brand at five measuring spray axial distances (Fig. 7).

This result was due to the fact that droplets were blended and ran along the original motion trajectory after the liquid film was broken twice, thereby forming stable droplet groups. Evaporation of the droplets could be ignored through the measurement ranges. As a result, droplet size hardly changed along the spray axial distance and was independent of spray axial distance. Therefore, the average droplet size at the five measuring positions under the same conditions can be considered the droplet size in subsequent research.

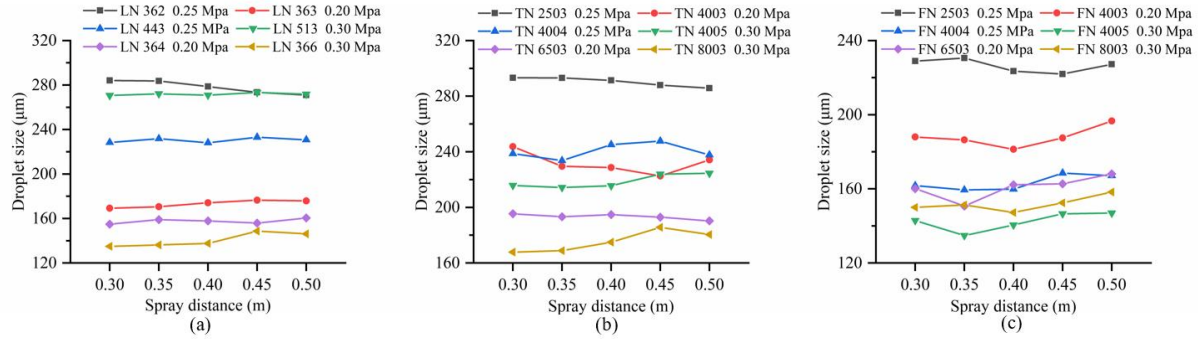

Fig. 7 - The relationship between droplet size and spray distance

Spray axial droplet size decreased as spray angle increased (Fig. 8). This phenomenon was due to the widening range of the fan liquid film as spray angle increased, forming more droplets that were smaller in size at the same flow rate and pressure. The fitting function of spray angle and axial droplet size was as follows:

$$D_v = (1 + a_v * \exp(-\alpha / 10)) \tag{14}$$

Where a_V was 18.00 for LN and 7.5 for TN and FN. Fitting degrees of the axial droplet size and spray angle are provided (Table 6).

Table 6

Fitting degrees of axial droplet size and spray angle

Parameter	LN 0.20 MPa	LN 0.25 MPa	LN 0.30 MPa
R^2	0.959	0.985	0.965
Parameter	TN 0.20 MPa	TN 0.25 MPa	TN 0.30 MPa
R^2	0.935	0.962	0.931
Parameter	FN 0.20 MPa	FN 0.25 MPa	FN 0.30 MPa
R^2	0.966	0.993	0.969

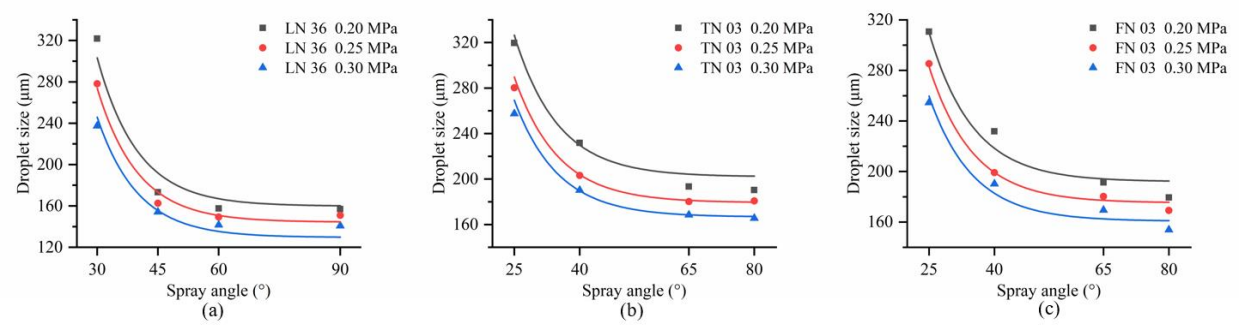

Fig. 8 - Fitting curves of droplet size and spray angle

Axial droplet size gradually decreased as pressure increased (Fig. 9). According to formulas (8) and (9), nozzle outlet velocity increased as nozzle inlet pressure increased, and the liquid film subsequently broke to produce smaller droplets. The fitting function of spray axial droplet size and pressure by fitting was as follows:

$$D_v = P^{b_v} \tag{15}$$

Where b_V was -0.30 for LN and TN and -0.40 for FN. Fitting degrees of axial droplet size and spray pressure are provided (Table 7).

Table 7

Fitting degrees of axial droplet size and spray pressure

Parameter	LN 362	LN 363	LN 443	LN 513	LN 364	LN 366
R^2	0.795	0.998	0.979	0.989	0.938	0.935
Parameter	TN 2503	TN 4003	TN 4004	TN 4005	TN 6503	TN 8003
R^2	0.930	0.946	0.998	0.987	0.964	0.921
Parameter	FN 2503	FN 4003	FN 4004	FN 4005	FN 6503	FN 8003
R^2	0.953	0.905	0.984	0.958	0.876	0.957

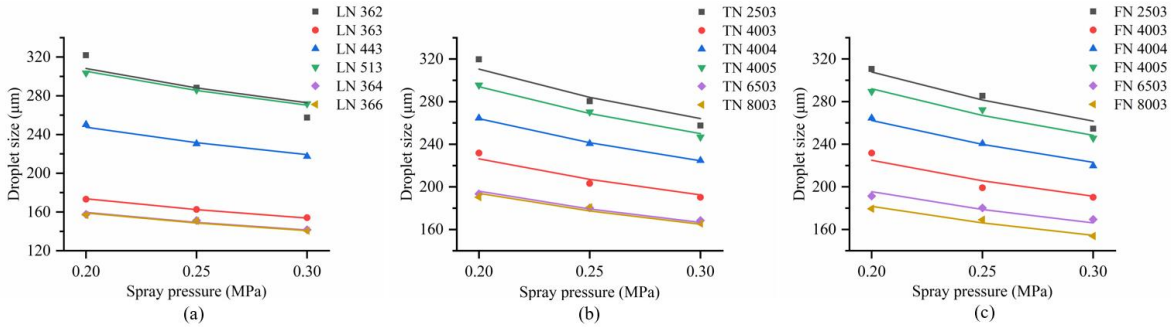

Fig. 9 - Fitting curves of droplet size and spray pressure

The relationship between the equivalent orifice diameter and spray axial droplet size at three pressures in the 16 nozzles was investigated at a spray angle of 40° for LN and 45° for TN and FN. Spray axial droplet size was positively correlated with the equivalent orifice diameter (Fig. 10). The fitting function of the spray axial droplet size and equivalent orifice diameter by fitting was as follows:

$$D_v = d^{c_v} \tag{16}$$

Where c_V was 0.95 for LN, 0.82 for TN and 1.10 for FN. Fitting degrees of axial droplet size and the equivalent orifice diameter are provided (Table 8).

Table 8

Fitting degrees of axial droplet size and the equivalent orifice diameter

Parameter	LN 0.20 MPa	LN 0.25 MPa	LN 0.30 MPa
R^2	0.970	0.985	0.987
Parameter	TN 0.20 MPa	TN 0.25 MPa	TN 0.30 MPa
R^2	0.985	0.983	0.994
Parameter	FN 0.20 MPa	FN 0.25 MPa	FN 0.30 MPa
R^2	0.967	0.964	0.969

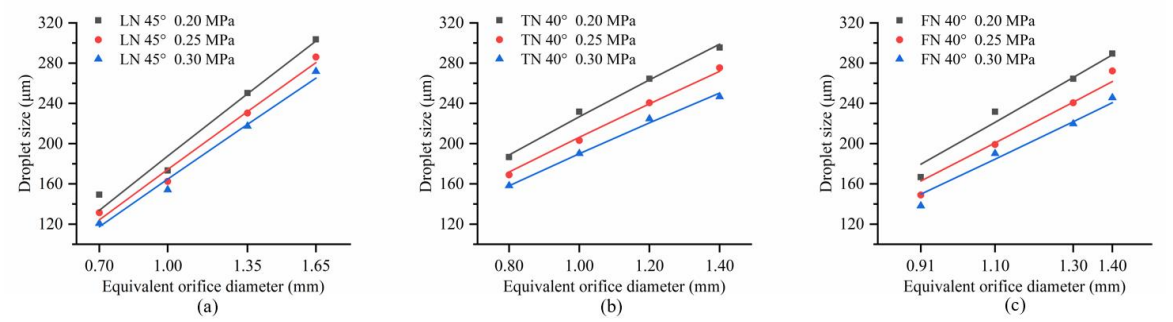

Fig. 10 - Fitting curves of axial droplet size and the equivalent orifice diameter

The following formula for spray axis droplet size was obtained from formulas (14)–(16):

$$D_v = (1 + a_v \exp(-\alpha / 10)) P^{b_v} d^{c_v} \quad (17)$$

The parameter values of different nozzle brands in the formula are provided (Table 9).

Table 9

Parameter values of the droplet size formula

Parameter	LN	TN	FN
a_v	18.00	7.50	7.50
b_v	-0.30	-0.40	-0.40
c_v	0.95	0.82	1.10

Validation

In order to ensure the accuracy of the axial droplet velocity and size model, the aforementioned parameters were calculated using formulas (13) and (17); the axial droplet velocity and size distribution curves of the three brands of nozzles were subsequently obtained (Fig. 11 and 12): (T) represents the theoretical data, and (A) represents the actual measured data. The results showed that the actual measured data were generally smaller than the theoretical data for velocity, and were two orders of magnitude larger for droplet size. The average absolute and relative errors for droplet velocity and size of the three brands are provided (Table 10). Although the theoretical data were larger or smaller than the actual measured data, the trends of the measured and theoretical data were roughly the same. This phenomenon was due to the liquid characteristics, design and processing of the nozzles, as well as air resistance and entrainment effects of the droplets during flight. Additionally, droplet velocity and size could be enlarged or reduced when multiplying the obtained formulas by fitting different parameters. For axial droplet size, the most important explanatory factor for theoretical droplet size was much smaller than the actual data because the direct relationship between axial droplet size and the liquid characteristics of the nozzle outlets was not established. Therefore, formulas (13) and (17) should be appropriately compensated to ensure that the theoretical values are closer to the actual values.

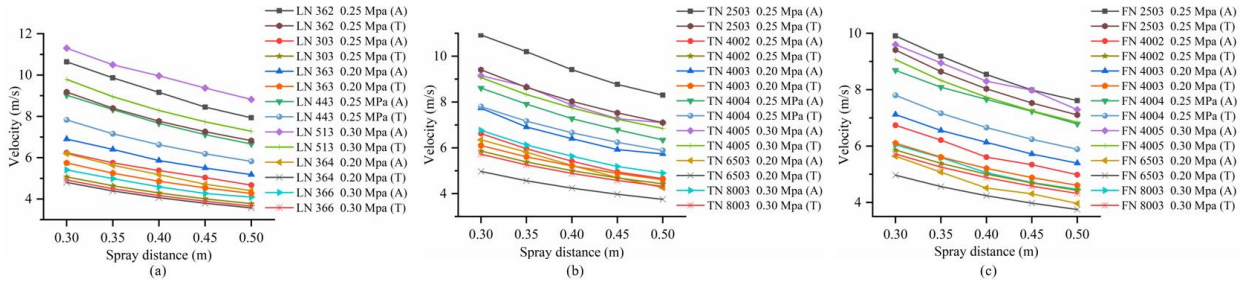

Fig. 11 - Comparison between the actual and theoretical axial velocities before compensation

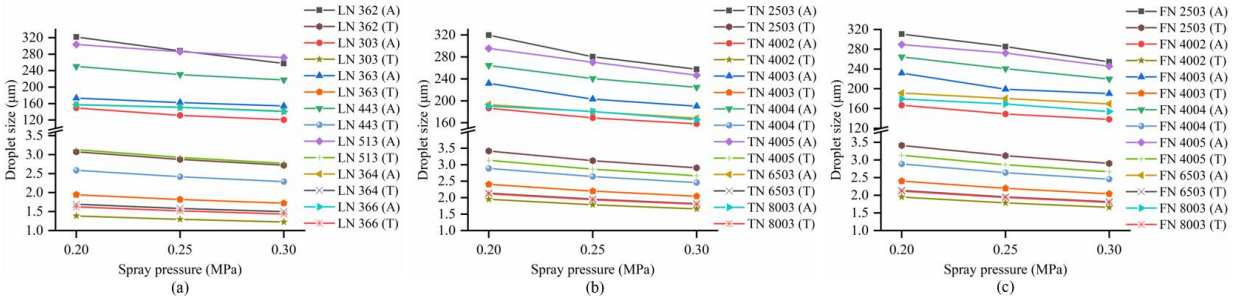

Fig. 12 - Comparison between the actual and theoretical axial droplet sizes before compensation

Table 10

The absolute and relative errors of droplet velocities and sizes before compensation

Manufacturer	Droplet velocity		Droplet size	
	Absolute error (m/s)	Relative error	Absolute error (μm)	Relative error
LN	1.071	14.49%	331.188	99.43%
TN	0.954	13.74%	339.385	99.49%
FN	1.151	17.24%	327.975	99.53%

By comparing the actual and theoretical data, the compensation values of the axial droplet velocities and sizes (i.e., C_m and C_v, respectively) of the three brands of nozzles based on spray angle were obtained (Table 11). Five nozzles of each brand were selected to validate the axial droplet velocity and size model. The comparison between the compensated and measured data is presented (Fig. 13 and 14), of which (TO) represents the compensated theoretical data. After compensation, the average absolute and relative errors for droplet velocity and size of the three brands are provided (Table 12). Therefore, the compensation values were reasonable and effective. The axial droplet velocity and size formulas are as follows:

$$u_m = C_m \left(2P/\rho\right)^{0.5} z^{a_m} \exp(b_m + c_m/\alpha) d^{d_m} \quad (18)$$

$$D_v = C_v (1 + a_v \exp(-\alpha/10)) P^{b_v} d^{c_v} \quad (19)$$

Table 11

Compensation coefficients of the theoretical formulas for the three nozzle brands

Parameter	LN				TN				FN			
	30°	45°	60°	90°	25°	40°	65°	80°	25°	40°	65°	80°
C_m	0.86	0.83	0.80	0.90	0.86	0.91	0.82	0.86	0.94	0.88	0.91	0.95
C_v	100	96	94	97	90	94	91	90	89	90	91	84

The average absolute and relative errors of the axial droplet velocity and size of the three brands of nozzles after compensation are provided (Table 12).

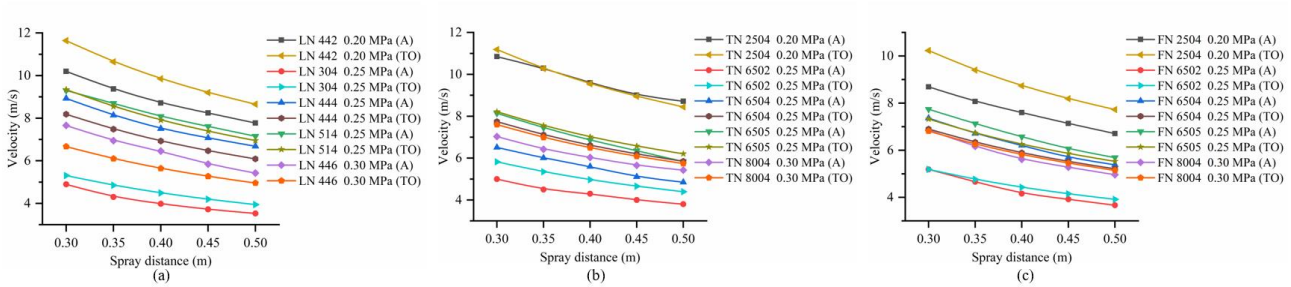

Fig. 13 - Comparison between the actual and theoretical axial droplet velocities after compensation

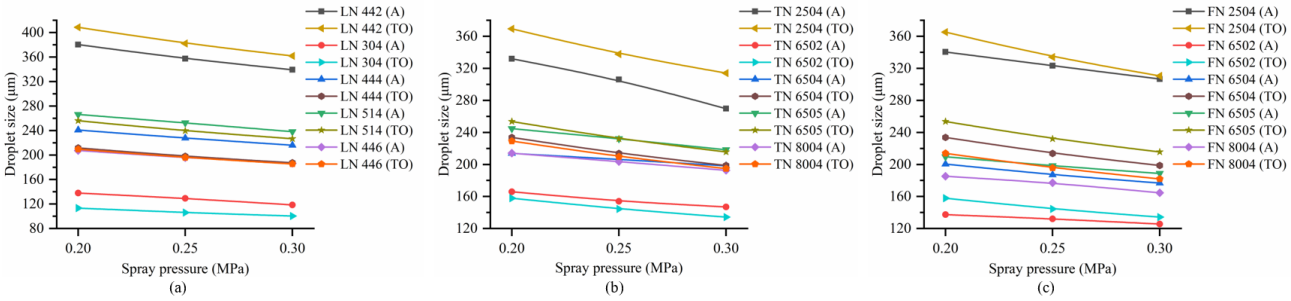

Fig. 14 - Comparison between the actual and theoretical axial droplet sizes after compensation

Table 12

The average absolute and relative errors for droplet velocities and sizes after compensation

Manufacturer	Droplet velocity		Droplet size	
	Absolute error (m/s)	Relative error	Absolute error (μm)	Relative error
LN	0.629	9.22%	17.821	8.40%
TN	0.521	9.60%	13.801	5.82%
FN	0.684	11.89%	22.140	11.67%

CONCLUSIONS

Based on the theoretical derivations and actual tests, this study established an axial droplet velocity and size model of the flat fan nozzle for agriculture and forest. Results revealed that the maximum average absolute and relative errors of the droplet velocity model were 0.684 m/s and 11.89%, respectively. The maximum average absolute and relative errors of the droplet size model were 22.140 μm and 11.67%, respectively. Thus, the theoretical atomization model was suitable and matched the actual test results.

Additionally, this study indicated that spray distance and spray angle were negatively correlated with axial velocity. There was a negative correlation detected between spray angle, pressure, and the axial droplet size. Axial droplet size was positively correlated with the equivalent orifice diameter. Moreover, the axial droplet size remained unchanged as spray distance increased within the spray range of 0.30–0.50 m. Thus, larger spray distances and spray angle should be selected at the same pressure. Although the axial droplet velocity and size models for the three brands of nozzles had the same functional form, the parameters were different, which may be due to the machining error and the different design standards.

ACKNOWLEDGMENTS

This research was supported by the National Natural Science Foundation of China (No. 31600588) and the National Key R&D Program of China (No.2018YFD0700603).

REFERENCES

[1] Chen G., Gu Y., Tsang H., (2018), The effect of droplet sizes on overspray in aerosol-jet printing. *Advanced Engineering Materials*, Vol.20, Issue 8, pp. 1701084, Germany;

[2] Geng L., Wang Y., Wang J., (2020), Numerical simulation of the influence of fuel temperature and injection parameters on biodiesel spray characteristics. *Energy Science & Engineering*, Vol.8, Issue 2, pp.312-326, USA;

[3] Ghate K., Sundararajan T., (2019), Effects of orifice divergence on hollow cone spray at low injection pressures. Proceedings of the Institution of Mechanical Engineers, Part G: *Journal of Aerospace Engineering*, Vol.233, Issue 11, pp.4091-4105, USA;

[4] Hinze J.O., (1955), Fundamentals of the hydrodynamic mechanism of splitting in dispersion processes, *Aiche Journal*., Vol.1, Issue 3, pp.289-295, USA;

[5] Jiang Y., Li H., Hua L., (2019), Experimental study on jet breakup morphologies and jet characteristic parameters of non-circular nozzles under low-intermediate pressures. *Applied Engineering in Agriculture*, Vol.35, Issue 4, pp.617-632, USA;

[6] Kang F., Pierce F. J., Walsh & D.B., (2011), An automated trailer sprayer system for targeted control of cutworm in vineyards. Trans. *ASABE*, Vol.55, Issue 5, pp.2007-2014, USA;

[7] Kang F., Wang Y., Li S., (2018), Establishment of a static nozzle atomization model for forest barrier treatment. *Crop Protection*, Vol.112, pp.201-208, England;

[8] Kooij S., Sijs R., Morton M.D., (2018), What determines the drop size in sprays? Physical Review X. Vol.8, Issue 3, pp. 031019, USA;

[9] Patel M.K., Praveen B., Sahoo H. K., (2017), An advance air-induced air-assisted electrostatic nozzle with enhanced performance. *Computers and Electronics in Agriculture*, Vol.135, pp.280-288, England;

[10] Preftakes C. J., Schleier J., Kruger G. R., Weaver, D. K., Peterson, R. K., (2019), Effect of insecticide formulation and adjuvant combination on agricultural spray drift. PeerJ, Vol. 7, pp. e7136, England;

[11] Sforza P. M., Steiger M. H., Trentacoste N., (1966), Studies on three-dimensional viscous jets. *AIAA JOURNAL*. Vol.4, Issue 5, pp.800-806, USA;

[12] Wang J., Zhou G., Wei X., (2019), Experimental characterization of multi-nozzle atomization interference for dust reduction between hydraulic supports at a fully mechanized coal mining face. *Environmental Science and Pollution Research*, Vol.26, Issue 10, pp.10023-10036, Germany;

[13] Wang S., He X., Song J., et al., (2018), Effects of xanthan gum on atomization and deposition characteristics in water and Silwet 408 aqueous solution. *International Journal of Agricultural and Biological Engineering*, Vol.11, Issue. 3, pp. 29-34, China.